applied sciences

MDPI

Article

CO_2 Distribution under CO_2 Enrichment Using Computational Fluid Dynamics Considering Photosynthesis in a Tomato Greenhouse

Moliya Nurmalisa [1], Takayuki Tokairin [1,*], Tadashi Kumazaki [2], Kotaro Takayama [3,4] and Takanobu Inoue [1]

[1] Department of Architecture and Civil Engineering, Toyohashi University of Technology, Toyohashi 4418580, Japan; moliya.nurmalisa.rc@tut.jp (M.N.); inoue.takanobu.zy@tut.jp (T.I.)
[2] Research Center for Agrotechnology and Biotechnology, Toyohashi University of Technology, Toyohashi 4418580, Japan; kumazak@recab.tut.ac.jp
[3] Department of Mechanical Engineering, Toyohashi University of Technology, Toyohashi 4418580, Japan; aa17091@gmail.com
[4] Faculty of Agriculture, Ehime University, Matsuyama 7908577, Japan
* Correspondence: tokairin.takayuki.gu@tut.jp

Abstract: This study validated the CO_2 distribution predicted by a computational fluid dynamics model considering CO_2 absorption by photosynthesis in a chamber and greenhouse. The effect of photosynthesis with CO_2 emission from a perforated tube remains not fully understood, although previous studies on CO_2 distribution in greenhouses have been conducted. Moreover, comparisons between CO_2 concentration measurement and simulation were obtained in the chamber and greenhouse model. Cases with open and closed side vents of the greenhouse showed that closed side vents have slightly more even of CO_2 concentration than those with open side vents inside the greenhouse. In contrast, the coefficient of variance (CV) of CO_2 inside the plant, open (8.8%) and closed (8.7%) side vents, induced almost no significant improvement. Additionally, cases of a rainy- and sunny-day model showed that photosynthetically active radiation possibly compensated CO_2 absorption through photosynthesis to be low at low light (rainy day) and higher at high light (sunny day). Nonetheless, the variability of CO_2 concentration inside the plant between rainy and sunny days determined almost no significant difference. Thus, this research shows characteristics of CO_2 distribution, assessing photosynthesis and the variability of CO_2 concentration that leads to the efficiency of CO_2 enrichment in the greenhouse.

Keywords: photosynthesis chamber; computational fluid dynamics; model validation; CO_2 enrichment; greenhouse

Citation: Nurmalisa, M.; Tokairin, T.; Kumazaki, T.; Takayama, K.; Inoue, T. CO_2 Distribution under CO_2 Enrichment Using Computational Fluid Dynamics Considering Photosynthesis in a Tomato Greenhouse. *Appl. Sci.* **2022**, *12*, 7756. https://doi.org/10.3390/app12157756

Academic Editor: José Carlos Magalhães Pires

Received: 23 June 2022
Accepted: 29 July 2022
Published: 1 August 2022

1. Introduction

Extending the farmland and improving production inside the greenhouse are two strategies expected to boost agricultural productivity. Many researchers have studied the microclimate phenomena of greenhouses because of the increasing demand for value-added agricultural products and the efficacy area of the greenhouse [1–3]. However, previous studies focused on the relationship between climatic factors that affect crop development [4–7]. In contrast, only a few studies have investigated the CO_2 distribution [8–11].

CO_2 enrichment is one of methods used to increase and distribute the CO_2 concentration near to the plant. This method is conducted by controlling and maintain CO_2 concentration inside the greenhouse [11]. It is challenging to maintain an optimal CO_2 concentration inside a greenhouse because CO_2 is affected by temperature, humidity, and light intensity, resulting in ambient CO_2 concentrations that are either suboptimal or excessive [12].

For example, Kuroyanagi et al. [13] investigated the amount of CO_2 that leaked from an unventilated greenhouse enriched with CO_2 on short-term (hourly) and medium-term

investigation. The average short-term CO_2 efficiency by crop absorption was 57.3% during the four days of daylight. For the medium term, more than 27 days, the efficiency of CO_2 enrichment was 45.5% on an average. The investigation demonstrated that the efficiency was not solely caused by the low levels of solar radiation or strong wind. In comparison, higher efficiency was achieved by higher solar radiation and weaker external wind.

Since CO_2 could not be homogeneously spread far from the CO_2 tube (CO_2 source), CO_2 distribution depends on air circulation inside the greenhouse. Thus, the delivery system (air circulation and ventilation) must be designed to ensure an even distribution throughout the greenhouse. Additionally, Kim et al. [14] showed that unequal distribution of CO_2 depends on temperature and location. A comparison showed that temperature is inversely proportional to the change in CO_2 distribution. As mentioned above, CO_2 enrichment plays a significant role in stable crop yield. Nevertheless, the detailed spatiotemporal distribution of CO_2 in foliage remains unknown.

Most of time, chambers are used in experiments to readily regulate environmental conditions because of their comparatively simple design. In this study, the performance of a recently constructed photosynthesis model for CO_2 distribution was assessed using a photosynthetic chamber with exhaust fans on top of the chamber. The new chamber is a semi-closed hanging type chamber covering the entire plant and monitoring the real-time photosynthetic rate.

The new chamber is shaped vertically because it is intended to completely cover plants, such as tomatoes. Shimomoto et al. [15] successfully tracked the time courses of tomato plants, the net photosynthetic rate, transpiration rate, and total conductance inside a monitoring system using a similar chamber. However, since measurement was conducted only for the photosynthetic rate and related environmental factors, the CO_2 distribution in the chamber was not well known.

Computational fluid dynamics (CFD) has been applied in various research areas to predict and simulate a similar process close to the actual condition. Many researchers have analyze greenhouse designs, airflow, temperature, and radiation distribution in the agricultural field using CFD [16–21]. Analysis of the detailed CO_2 distribution is rarely implemented and is still ongoing to date. Zhang et al. [11] showed that the efficiency of CO_2 distribution using CO_2 supplement/tube could save half of the fuel and achieve a higher CO_2 concentration compared with a CO_2 generator.

CFD is a powerful tool for describing greenhouse microclimate, plant behavior [22], and photosynthesis. Molina-Aiz et al. [9] reported that photosynthesis could be simulated accurately using CFD in each cell of the domain corresponding to the crop. In their study, photosynthesis was computed as a function of the CO_2 concentration estimated by the CFD software. The CFD model made it possible to reveal airflow details above and within the canopy, effects of the different structures on water irrigation, and predicted crop transpiration [23–25].

The validity of the CFD results has been a perennial problem. However, the continuous development of computer and numerical methods enhances the accuracy of the simulation prediction and shows outstanding potential for analyzing complex airflow in a greenhouse [20]. Although photosynthesis has been considered in a recent CFD model, analysis of CO_2 distribution by CO_2 enrichment and emitted by CO_2 supplement/tube is insufficient. Since this research is rarely conducted, this study focuses on finding detailed CO_2 distribution concerning the increased efficiency of photosynthesis.

The objective of this study is to reveal the detailed CO_2 distribution using a CFD model considering photosynthesis with CO_2 enrichment using CO_2 supplement/tube inside the greenhouse. First, the effectiveness of the model is assessed by comparing numerical simulations and measuring the CO_2 levels in the new chamber.

In the chamber simulation, the photosynthesis model is considered to simulate CO_2 absorption, and reasonable results for the model performance are obtained. Finally, the simulated CO_2 content is verified, and the photosynthesis model is used to calculate the precise CO_2 distribution with CO_2 enrichment inside the greenhouse. A few greenhouse

simulations are conducted to determine the impact of various environmental factors on the distribution of CO_2 inside of the greenhouse, including side vents that can be open or closed and weather conditions that can be sunny or rainy.

2. Materials and Methods

2.1. Experimental Set-Up

2.1.1. Chamber Description

The experiment was conducted in a chamber inside the greenhouse with a CO_2 concentration of approximately 420 ppm. The chamber is a semi closed hanging type that is 1 m in length, 0.52 m in width, 1.64 m in height, and an area of the bottom opening: 0.52 m^2 (1 m in length × 0.52 m in width) (Figure 1). The air inside the chamber flows out through an exhaust fan (9BMB24P2H01, Sanyo Denki, Philippines) at the left ceiling of the chamber. The air velocity of the fan is 18.7 m s^{-1}, applied to determine the volumetric flow rate of the fan in this research and used in the simulation as shown below (Equation (1)):

$$Q = u_{out} \times A_{out} \quad (1)$$

where u_{out} is the air velocity at the exhaust fan boundary (m s^{-1}), Q is the outlet volumetric flow rate (m^3 s^{-1}), and A_{out} is the outlet opening area (m^2).

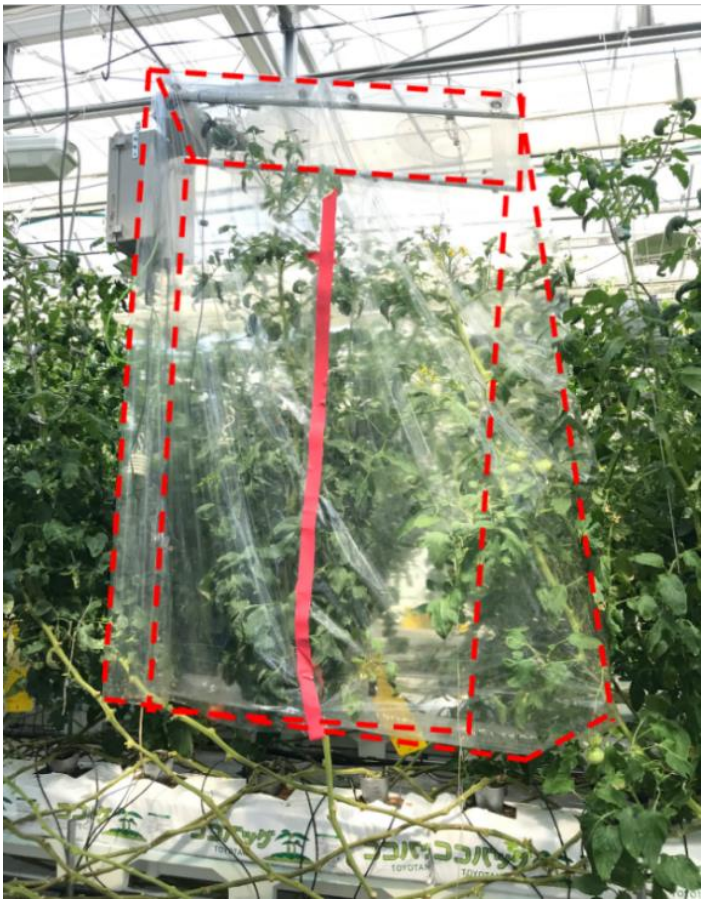

Figure 1. Chamber inside the greenhouse.

Two whole-grown tomatoes were placed inside the chamber in the substrate with a drip nutrient and irrigation system. The tomatoes had heights of 1.63 and 1.4 m, respectively, from the chamber bottom; leaf area index (LAI) of 4 m^2 m^{-2}; and leaf area density (LAD) of 2.67 m^2 m^{-3}. Later, in the chamber model validation, the average height of 1.5 m was used to represent the height of the plant.

2.1.2. CO_2 Distribution Measurement in the Chamber

CO_2 concentrations were measured using a handheld CO_2 m (GM70, probe type GMP 222, range 0–5000 ppm, accuracy: ±1.5% of range +2% of reading, Vaisala, Finland). The measurements of CO_2 concentration without CO_2 enrichment were conducted in three positions: top (0.15 m from the chamber ceiling), middle (0.815 m from the chamber ceiling), and bottom (at the bottom opening of the chamber) to obtain CO_2 distribution data for model validation. CO_2 concentration at each position was measured in three horizontal points (left, middle, and right) in the exact distance between the point is 0.25 m.

The CO_2 concentration at each point were measured with the CO_2 m held by hand and recorded manually to a sheet when the value displayed on the CO_2 m was stable. However, the CO_2 concentration of the top positions were measured at the left and right because of difficulty reaching the middle point while avoiding human breath exhaling CO_2. Air velocities were measured at the bottom of the chamber (0.83 m from the ground) and 0.2, 0.4, and 0.815 m from the ceiling of the chamber, using a hot wire anemometer (WGT 10, Hario, Japan) to determine the airflow and CO_2 distribution (Figure 2).

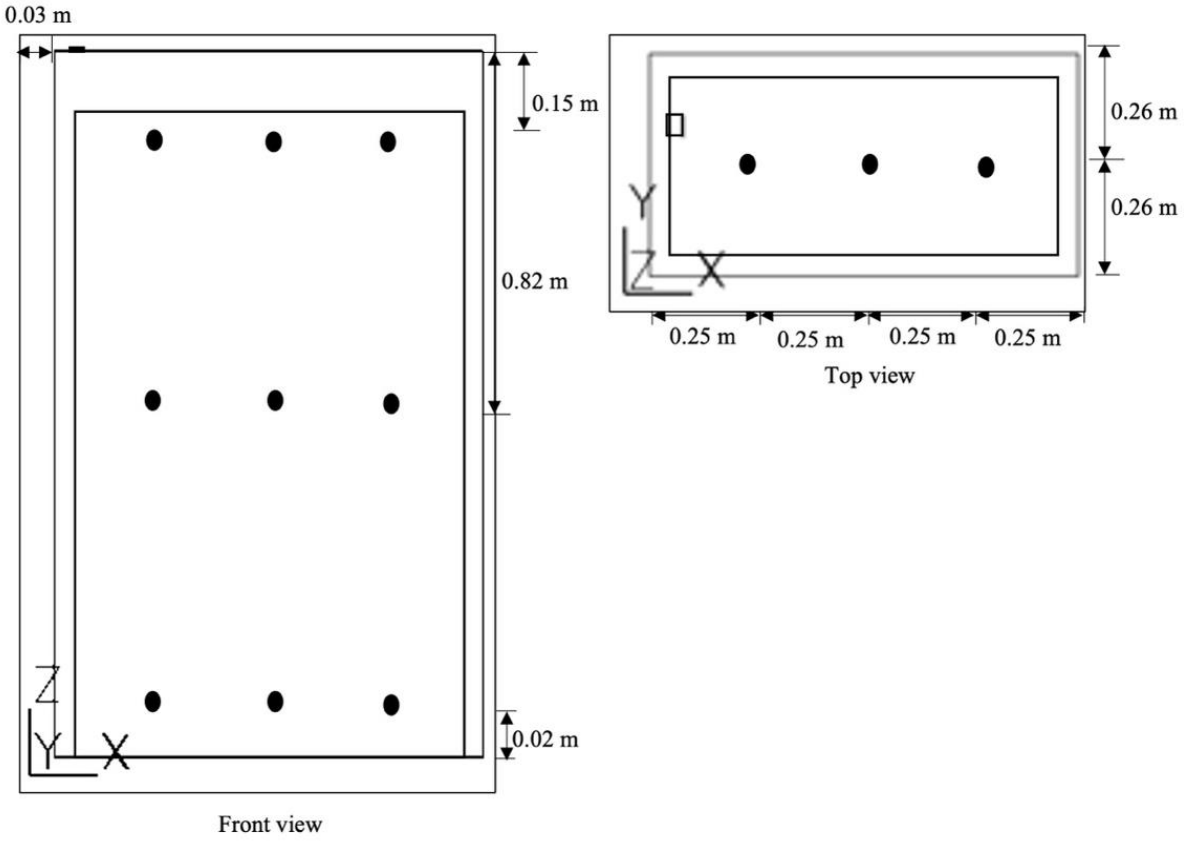

Figure 2. CO_2 measurement points (●) at the front (**left**) and top (**right**)-view.

2.1.3. Greenhouse Description

This study was conducted in a vinyl greenhouse of 120 m^2 (length: 12 m; width: 10 m; height: 6.03 m) located at Toyohashi University of Technology, Japan (Figure 3). The greenhouse was equipped with air conditioning, air circulators, roof and side vents, water and nutrient solution drip-irrigation system, and a perforated tube of airflow system placed above the bed of plants shelves. Additionally, the greenhouse's roof and side vents were covered with insect-proof nets.

Figure 3. The greenhouse for CO_2 measurement.

Tomatoes were grown on four shelves inside the greenhouse: tomato seedlings (Solanum lycopersicum), cv. 'Momotaro hope', was planted on 4 November 2020, in greenhouse. Tomatoes grow in the cultivated bed (0.23 m in width and 8 m in length), mounting 0.83 m from the ground floor. The water and nutrient solution supply are controlled using monitoring instruments (Aqua beat, Inochio, Japan). The solar radiation data were acquired from the NEDO database (New Energy and Industrial Technology Development Organization, Japan) to calculate PAR (Photosynthetically Active Radiation).

2.1.4. Measurement of CO_2 Concentration in Greenhouse

CO_2 enrichment was conducted during the daytime on a sunny day (on 30 August 2021, at 1.30 p.m.). The initial CO_2 concentration injection was 1160 ppm. Pure CO_2 gas was supplied through a perforated tube airflow system placed in the middle of the bed of plants for each shelf. The perforated tube has a length of 8 m, a diameter of 0.10 m, and 16 holes with a diameter of 0.006 m, and the distance between the hole is 0.52 m.

The average air velocity of the outlet perforated tube airflow system was 6.21 m s^{-1}. CO_2 gas was flowing from north to south in the perforated tube. CO_2 gas from the perforated tube hole was measured after less than 5 min of injection of CO_2 gas. CO_2 concentrations were measured using a handheld CO_2 m (GM70 probe type GMP 222, range 0–5000 ppm, accuracy: ±1.5% of range +2% of reading, Vaisala, Finland) within a 30 s average. This measurement data will be used for greenhouse simulation cases.

2.1.5. Brief Description of CO_2 Enrichment on CO_2 Distribution in a Greenhouse

Kumazaki et al. [26] studied influential positions of CO_2 supply in tomato plants inside the greenhouse. The tomato plants have LAI 1.1 m^2 m^{-2}. The CO_2 was supplied in two positions: (i) at the base of the canopy plant (0.6 m above the ground) and (ii) the middle canopy (1.2 m above the ground). CO_2 supply started when the CO_2 concentration average was below 400 ppm and stopped when it achieved 450 ppm. CO_2 concentrations were measured at 0.6, 1.2, 1.8, 2.4, and 4.2 m above the ground. As the CO_2 distribution in the entire greenhouse remains unclear, this study conducted a numerical simulation to predict the CO_2 distribution using CO_2 concentration measurement data. This measurement data obtained at 1.2 m height of CO_2 supply will be used for greenhouse model validation.

2.2. Numerical Modelling

CFD simulations were conducted using a commercial CFD software (PHOENICS, v.2020, CHAM Ltd., London, UK). The software solves the steady-state three-dimensional simulations using the finite volume method. Benni, et al. [2] explained that the finite volume method reduces the governing partial differential equations to a set of algebraic equations, resulting in algebraic equations for the dependent variable at nodes on every element. PHOENICS solves a finite volume formulation of the balance equation, which is unsolved in differential form [27]. The numerical simulation imposed the boundary conditions at the calculation domain to conduct airflow, CO_2 distribution, and photosynthesis processes.

2.2.1. Governing Equations

The continuity equations model (Equation (2)), momentum equations, and the energy equation applied to calculate airflow and heat transfer in this research are shown below:

$$\frac{\partial \rho}{\partial t} + \frac{\partial(\rho u)}{\partial x} + \frac{\partial(\rho v)}{\partial y} + \frac{\partial(\rho w)}{\partial z} = 0 \quad (2)$$

where ρ is the fluid density (kg m^{-3}); t is time (s); and u, v, and w are the air velocity components of the x, y, and z directions. The transport equation (Equation (3)), where ϕ represents the concentration of the transport variables, mass (air and CO_2 mass fraction), momentum, and energy [28].

$$\frac{\partial}{\partial t}(\rho\phi) + div(\rho u\phi) = div\left(\acute{\Gamma}_{\phi} grad\phi\right) + S_{\phi} \quad (3)$$

where ρ is the density, u is the component of directional air velocity, $\acute{\Gamma}_{\phi}$ is the diffusivity coefficient for ϕ, and S_{ϕ} is the source term.

Managing the meshing grid to obtain accurate simulation results was challenging. Hong et al. [20] discussed that finer meshes might not improve the accuracy anymore, whereas coarser meshes might still give accurate results for some cases.

2.2.2. Photosynthesis Model

PHOENICS automatically computes the mass fractions of CO_2 in the air. The net photosynthesis was calculated using the equation below (Equation (4)) as the difference between canopy photosynthesis and crop respiration.

The formula of net photosynthesis (kg s^{-1} m^{-3} $_{row}$) was given as follows [9]:

$$S_{CO_2} = -P_{cCFD} = \frac{LAD_r}{LAI \cdot 1000 \cdot 3600}\left(R' - P_{cg}\right) \quad (4)$$

where LAD is the leaf area density (m^2 m^{-3}), LAI is the leaf area index (m^2 m^{-2}), P_{cg} is canopy photosynthesis rate (g CO_2 h^{-1} m^{-2} ground area), R' is the crop respiration (g h^{-1} m^{-2}), and S_{CO_2} is the source or sink term.

Canopy photosynthesis rate of Acock's model modified by Nederhoff and Vegter [29] (Equation (5)):

$$P_{cg} = \frac{\alpha_c j_o \tau_c C' \cdot 3600}{\alpha_c j_{o+} \tau_c C'} \quad (5)$$

where α_c is the initial light use efficiency of the plant canopy (or light utilization or photosynthetic efficiency) (g CO_2 J^{-1}), j_o is the incident light flux, PAR at the top of the canopy (W m^{-2}), τ_c conductance to CO_2 transfer (m s^{-1}), C' is the concentration of CO_2 in the air which is calculated from the mass fraction of CO_2, YCO_2 (kg kg^{-1}), and the air density ρ (kg m^{-3}) [9].

In the chamber simulation, a simple rectangular plant object with a length of 0.4 m, a width of 0.9, and a height of 1.5 m were considered, respectively. The LAI and LAD were 4 m^2 m^{-2} and 2.67 m^2 m^{-3}. This study used LAI to calculate air velocity's deceleration in

the plant canopy. The deceleration is often represented as momentum sink (Equation (6)) in source term of Equation (3):

$$S_\varphi = C_D \alpha u^2 \tag{6}$$

where C_D is a drag coefficient of the crop (0.3), α denotes LAD (m^2 m^{-3}), and α is obtained from LAI (Equation (7)):

$$\alpha = \frac{LAI}{h} \tag{7}$$

where h is the plant canopy's height.

2.3. Model Settings and Validation

2.3.1. Chamber Model

The chamber model replicated the bottom open chamber. A similar chamber has been used to investigate photosynthetic rate, related environmental factors [15], and airflow uniformity [30]. Chamber dimensions of length, width, and height were 1, 0.52, and 1.64 m, respectively (Figure 4). In the calculation of chamber simulation, the scale of the domain was small and consisted of two plants and one fan as outlet and inlet at the bottom part of the chamber.

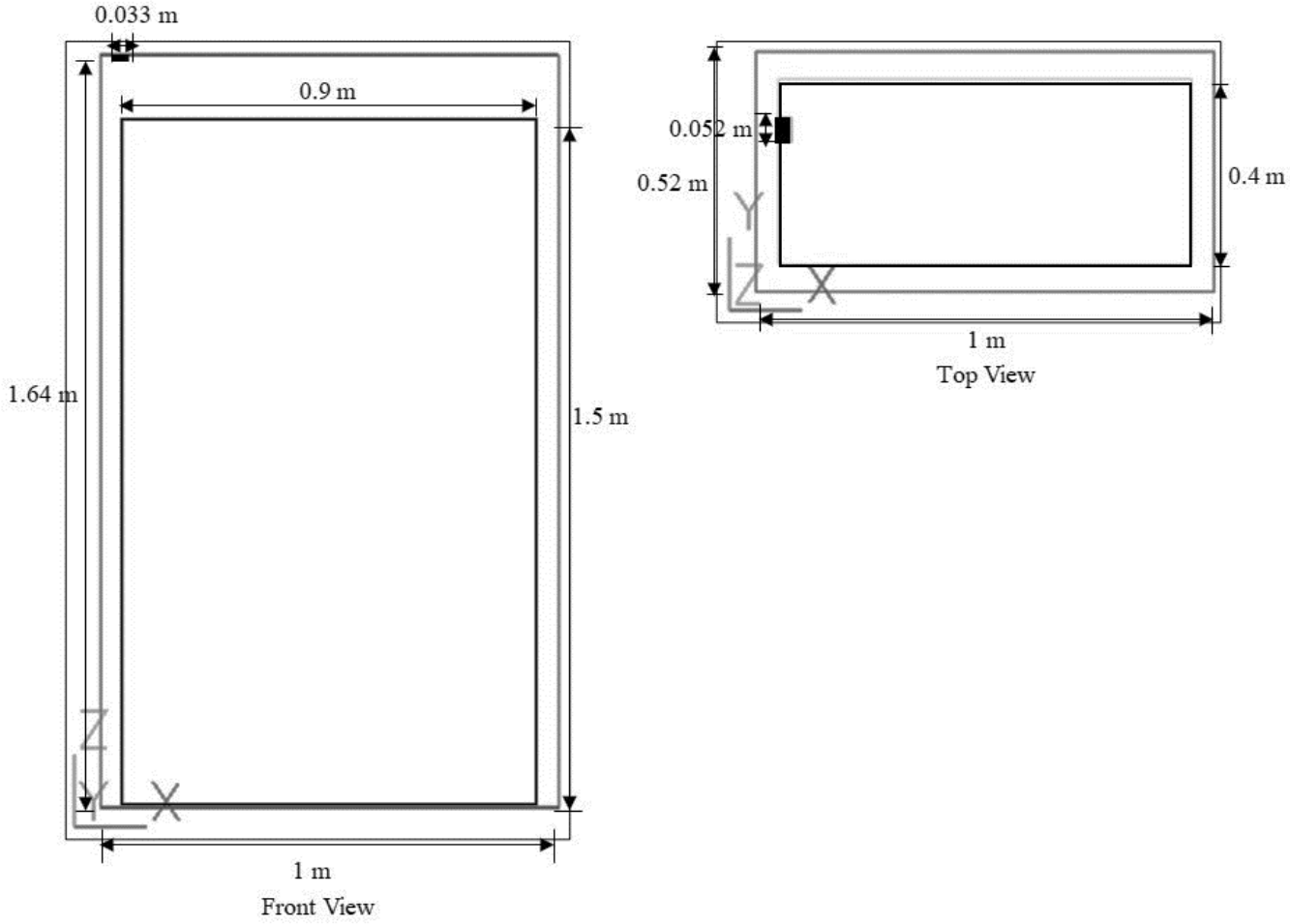

Figure 4. Chamber model: Fans are placed at the top left side of the chamber (▬ represents the fan). The rectangular shape inside of the chamber represent the plant.

The CO_2 distribution model used in chamber simulation was the laminar flow model. In the calculation of chamber simulation, the scale of the domain was compact but sufficient to calculate canopy photosynthesis for the whole body of the tomato plant. The mesh numbers in the computational domain had 5940 cells inside the chamber (Figure 5). Cham-

ber simulation has been conducted to investigate CO_2 distribution and photosynthesis, particularly net photosynthesis rate. The initial CO_2 concentration for the simulation was set at 450 ppm, which is same as the measured from the outlet of bottom chamber.

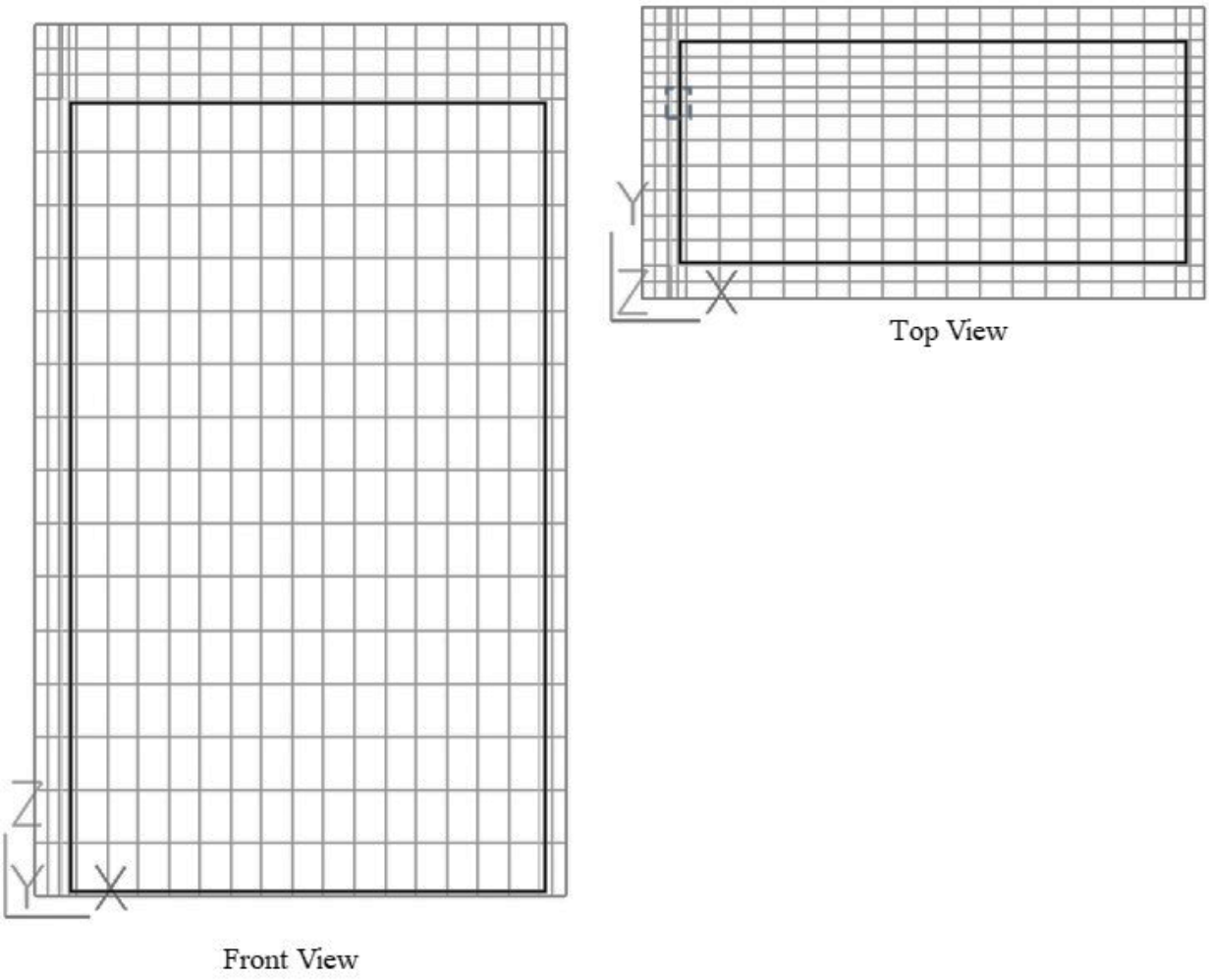

Figure 5. Meshing of chamber model: the dashed line square at top view represents fan ( ). The rectangular shapes inside of the chamber represent the plants.

2.3.2. Validation Chamber Model

This study conducted a chamber simulation, compared the measurement data, and analyzed the CO_2 concentration in three measurement positions in the chamber. The model validation was performed using three positions of CO_2 concentration: (i) above the plant and near the fan, (ii) in the middle of the plant, and (iii) at the bottom of the chamber near the area of inflow air from the outer chamber. Those positions were chosen to be representative of the characteristics of airflow in the whole chamber, including plants with photosynthesis process.

A validated chamber model will be applied to simulate the actual greenhouse. The root-mean-square error (RMSE) and mean absolute percentage errors (MAPE) for each point between the measured and simulated data were used to assess the simulation model's accuracy [1]. The computational configuration for the three-dimensional CFD simulation is presented in Table 1.

Table 1. Computational conditions used for the chamber model.

Parameter	Symbol	Unit	Value
Canopy photosynthesis rate	P_{cg}	g CO_2 h^{-1} $m^{-2}_{ground\ area}$	
CO_2 density	Cc	g m^{-3}	1839
Conductance of CO_2	τ_c	m s^{-1}	12.168×10^{-4}
Crop respiration	R′	g $h^{-1}m^{-2}$	2.84×10^{-2}
Initial CO_2	-	ppm	450
Leaf area density	LAD/α	m^2_{leaf} m^{-3}_{row}	2.67
Leaf area index	LAI	m^2 m^{-2}	4
The light use efficiency of the plant canopy	α_c	g CO_2 J^{-1}	3.705×10^{-6}
The incident light flux PAR	J_o	W m^{-2}_{leaf}	379.9

2.3.3. Greenhouse Model

The computational model greenhouse has dimensions of length 12 m, width 10 m, and height 6 m. The greenhouse model has four circulating fans, four shelves of cultivating bed for tomato, and four CO_2 perforated tubes on each shelf (Figure 6). Leakage paths were managed in the door area and for tiny gaps across the greenhouse rib structure between the wall and the roof [31].

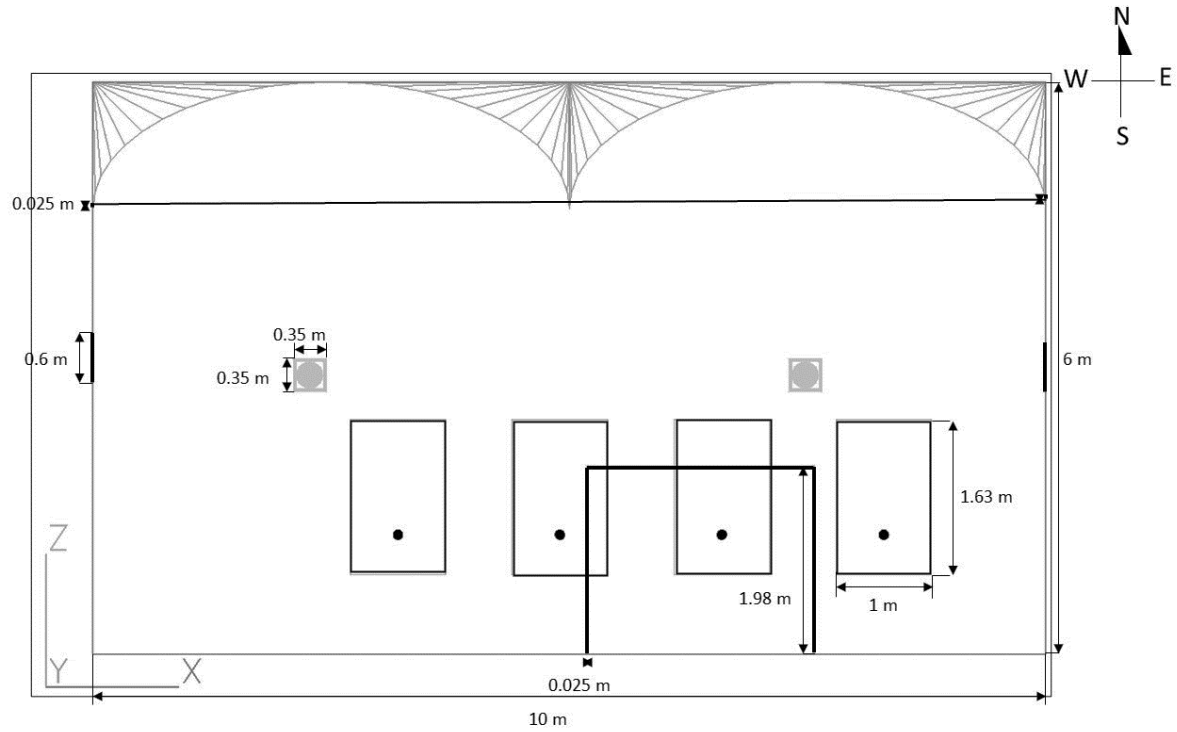

Figure 6. Greenhouse model: (the squares represent fan circulator, rectangular shapes represent the plants, the circles represent CO_2 perforated tube, and the thick lines and dots represent outlet).

Several turbulence models were tested to adopt suitable turbulence models in the greenhouse [5,32]. Natural ventilation of the greenhouse simulation was validated by different mesh sizes and different turbulence models to determine the accuracy of CFD simulation [20]. This study tested different turbulence models to simulate CO_2 distribution while considering CO_2 absorption by the photosynthesis process and found that the optimum convergence was achieved in the standard $k-\varepsilon$ turbulence model. Accordingly, the standard $k-\varepsilon$ turbulence model was applied in the greenhouse simulation.

2.3.4. Validation of the Greenhouse Model

The greenhouse simulation was conducted and compared with the measurement data of CO_2 enrichment. Model validation calculated the CO_2 distribution from CO_2 perforated tubes in the whole greenhouse. The number of meshes in the computational domain had 739,350 cells inside the greenhouse (Figure 7). The simulation model's accuracy was assessed using RMSE and MAPE by comparing the percentage errors of each measured and simulated point. Table 2 presents the computational conditions used for the three-dimensional CFD simulation.

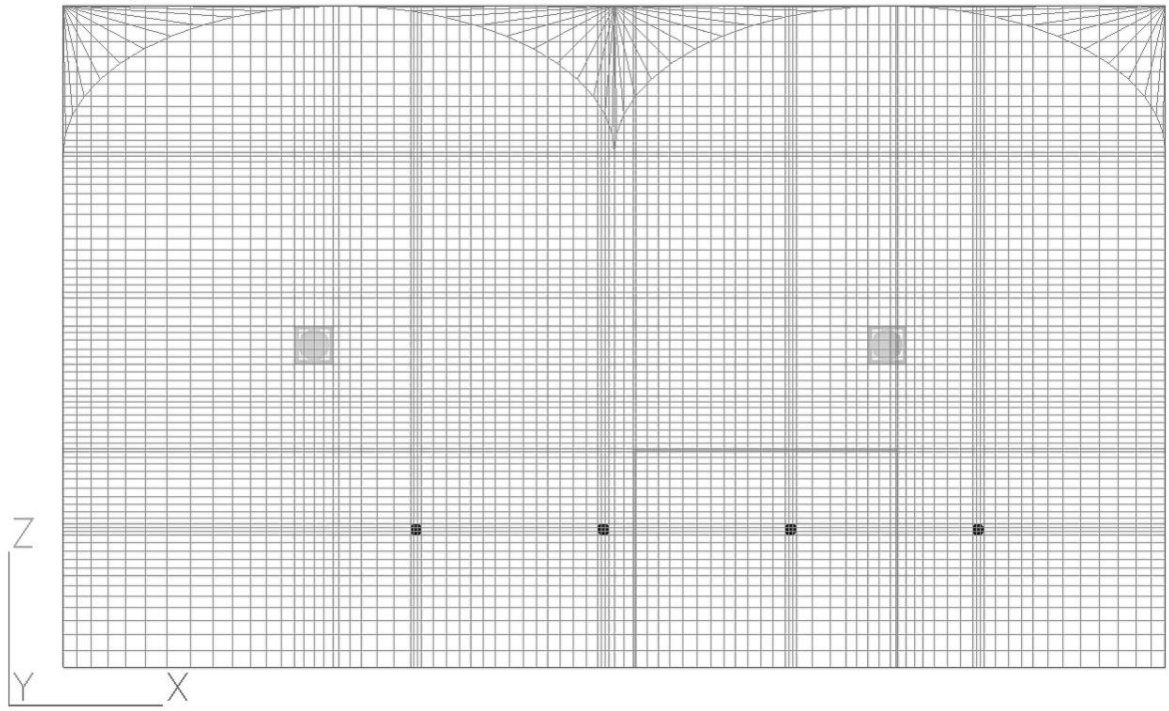

Figure 7. Meshing of greenhouse model: (the four rectangular shapes inside the chamber represent the plants, the circles represent CO_2 perforated tube, and the squares represent fans).

Table 2. Computational conditions used for greenhouse model.

Parameter	Symbol	Unit	Value
Canopy photosynthesis rate	P_{cg}	g CO_2 h^{-1} $m^{-2}_{\text{ground area}}$	
CO_2 density	Cc	g m^{-3}	1839
Conductance of CO_2	τ_c	m s^{-1}	12.168×10^{-4}
Crop respiration	R'	g h^{-1} m^{-2}	2.84×10^{-2}
Initial CO_2	-	ppm	450
Leaf area density	LAD/α	m^2_{leaf} m^{-3}_{row}	0.67
Leaf area index	LAI	m^2 m^{-2}	1.1
The light use efficiency of the plant canopy	α_c	g CO_2 J^{-1}	3.705×10^{-6}
The incident light flux PAR	J_o	W m^{-2}_{leaf}	355

Using a coefficient of variation (CV), the variability of CO_2 distribution inside the greenhouse was examined for two types of scenario cases, open and closed side ventilation and weather (rainy and sunny days). The 7070 points of CO_2 concentration were taken to measure the variability inside the greenhouse and 8484 points of CO_2 concentration for plants.

Note that the measurements of CO_2 concentration for chamber and greenhouse have been carried out at different date (4 August 2021, for CO_2 concentration measurement at chamber and 30 August 2021, for CO_2 concentration measurement at greenhouse that will be used for simulation cases). The data of LAI and some parameters that used in model were the data at the date of CO_2 measurement. Due to this, some parameters are different between the chamber and greenhouse.

3. Results and Discussion

3.1. Model Validation

3.1.1. CO_2 Distribution Inside the Chamber

The measured CO_2 concentrations were compared with the simulated CO_2 distribution inside the chamber. Model simulation accuracy was evaluated by comparing each measured and simulated point's percentage errors of Table 3. The MAPE of the left, middle, and right parts of the chamber were 1.85%, 3.43%, and 0.43%, respectively, and the RMSE of left, middle, and right parts were 11.20, 16.99, and 2.17 ppm, respectively, according to the CFD model for CO_2 distribution.

Table 3. Comparison of CO_2 concentration between measured and simulated data for model validation in the chamber.

Canopy Layer	Measured			Simulation			Percentage error (%)		
	Left	**Middle**	**Right**	**Left**	**Middle**	**Right**	**Left**	**Middle**	**Right**
Top	420	–	440	439	442	442	4.53	–	0.36
Middle	440	420	440	444	443	443	0.84	5.59	0.76
Bottom	450	455	450	449	449	449	0.17	1.27	0.17
MAPE (%)	1.85	3.43	0.43						
RMSE (ppm)	11.20	16.99	2.17						

The results showed that employing a tomato plant as a porous medium considered the photosynthetic process could reasonably predict CO_2 distribution. In comparison to the actual canopy of the tomato plant, the model tomato plant has been simpler. That is, the dense leaves were considered homogenous for the entire plant. Thus, the CO_2 concentration shows a decrease inside the porous medium (corresponding to tomato plant), where the air, including CO_2, may go through the canopy of the tomato plant; then, the CO_2 is absorbed by the process of photosynthesis (Figure 8).

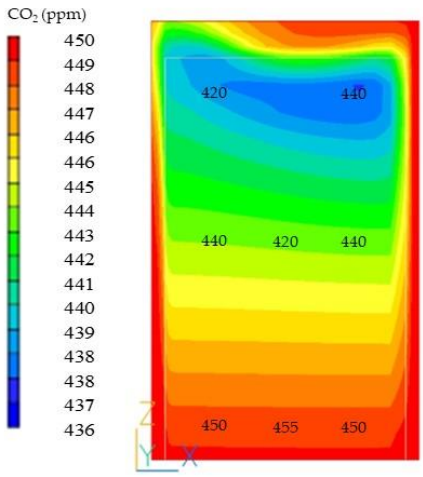

Figure 8. The CO_2 distribution inside the chamber: The values are the measured data of the CO_2 concentration.

The CO_2 concentration distribution according to the chamber measurement and simulation for each height were compared to evaluate numerical simulation properties (Figures 8 and 9). These figures showed the simulation results of CO_2 concentration at the left and middle part were slightly overestimated. However, the simulation was still reasonable and can be used for greenhouse numerical simulation.

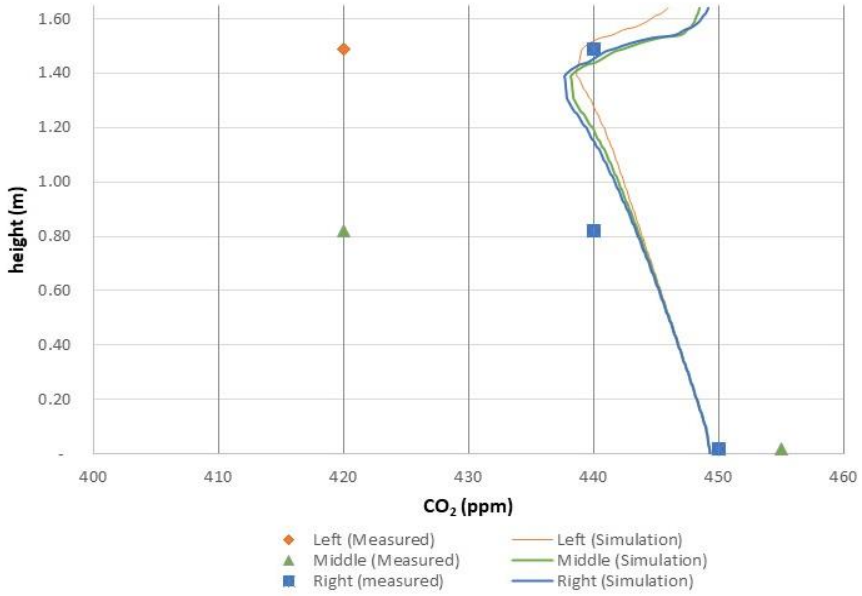

Figure 9. Measured and simulated data of CO_2 concentration inside the chamber.

3.1.2. CO_2 Distribution Inside the Greenhouse

The greenhouse model validation was conducted according to the measurement data of Kumazaki, et al. [26], who studied influential positions of CO_2 supply in tomato plants inside the same greenhouse as the present study. In the present study, the simulation results were compared with the measurement data of CO_2 concentration in the condition 20 min after 1 h of CO_2 being supplied at the middle canopy (1.2 m above the ground, see Figure 10).

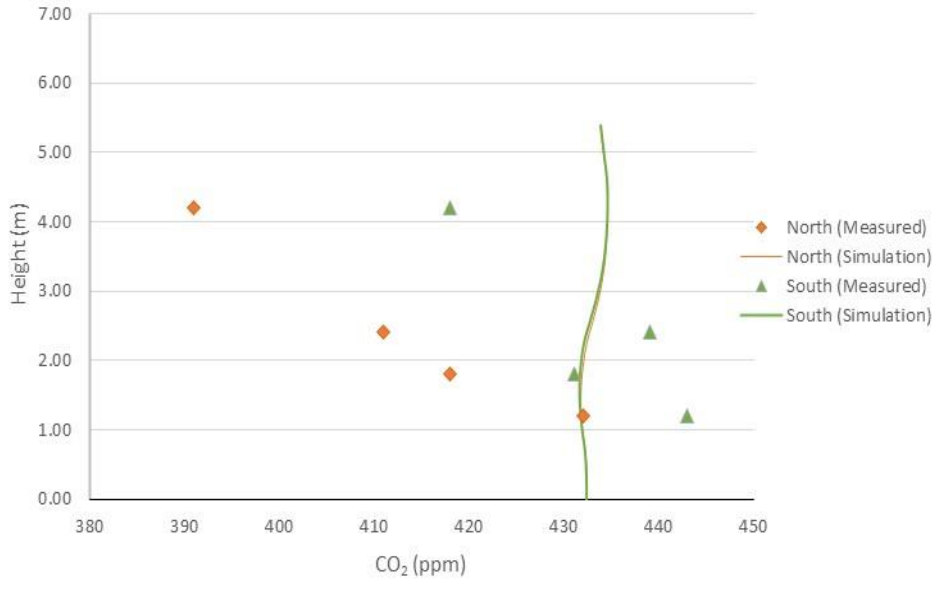

Figure 10. CO_2 concentration of measurement (north ♦ and south ▲) and simulation (north and south –) data according to the position from the ground.

The CO_2 concentrations were measured at two sides of 3.4 m from the north and south wall with 0.6, 1.2, 1.8, 2.4, and 4.2 m above the ground. The initial simulation value of CO_2 concentration was assumed to be constant in every mesh inside the greenhouse, whereas the actual condition has various CO_2 concentrations. In contrast, model simulation accuracy was also evaluated by comparing the percentage errors of each measured and simulated point (Table 4).

Table 4. Comparison of CO_2 concentration between measured and simulated data for model validation in greenhouse.

Height (m)	Measured (ppm)		Simulation (ppm)		Percentage Error (%)	
	North	South	North	South	North	South
4.2	391	418	435	435	11.15	3.96
2.4	411	439	433	432	5.28	1.53
1.8	418	431	432	432	3.34	0.14
1.2	432	443	432	432	0.03	2.55
MAPE (%)	4.95	2.04				
RMSE (ppm)	25.33	10.57				

According to the results of the CO_2 distribution using the CFD model within the greenhouse, the MAPE of north and south were 4.95% and 2.04%, respectively, whereas the RMSE of north and south were 25.33 and 10.57 ppm, respectively, compared with the measured values. However, the simulation results in this study may be reasonable to predict the CO_2 distribution considering CO_2 absorption through the process of photosynthesis of the plant inside the greenhouse (Figure 11).

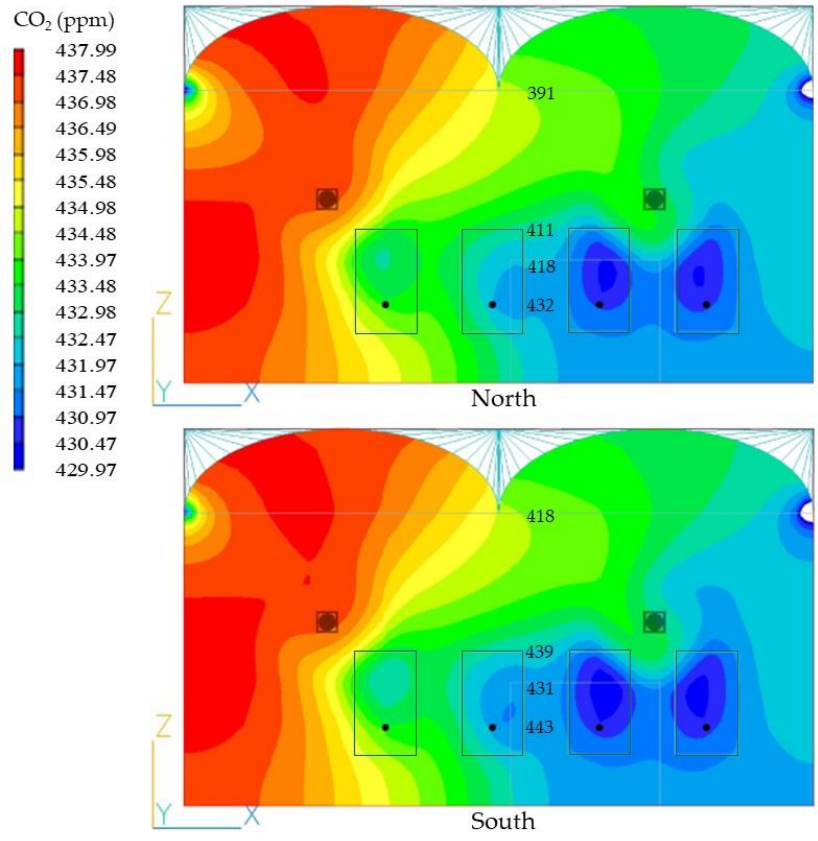

Figure 11. CO_2 distribution inside the greenhouse considering CO_2 absorption through photosynthesis by plants (image taken at cross-section 3.4 m from south wall).

3.2. Simulation Cases for Greenhouse Model

Several simulations were conducted to analyze CO_2 distribution under the CO_2 enrichment described below. The cases were trial scenarios to determine the detailed CO_2 distribution while considering the photosynthesis process inside the greenhouse.

3.2.1. CO_2 Distribution toward Open and Closed Side Ventilation Inside the Greenhouse

Figure 11 shows the simulation of CO_2 distribution inside the greenhouse when 1160 ppm CO_2 concentration was supplied through perforated tubes inside the plants. The appearance of CO_2 emissions from the perforated tube was confirmed with the degradation colors inside of the plants. CO_2 distribution in case open and closed side vents were showed a slight difference in CO_2 concentration (Figure 12).

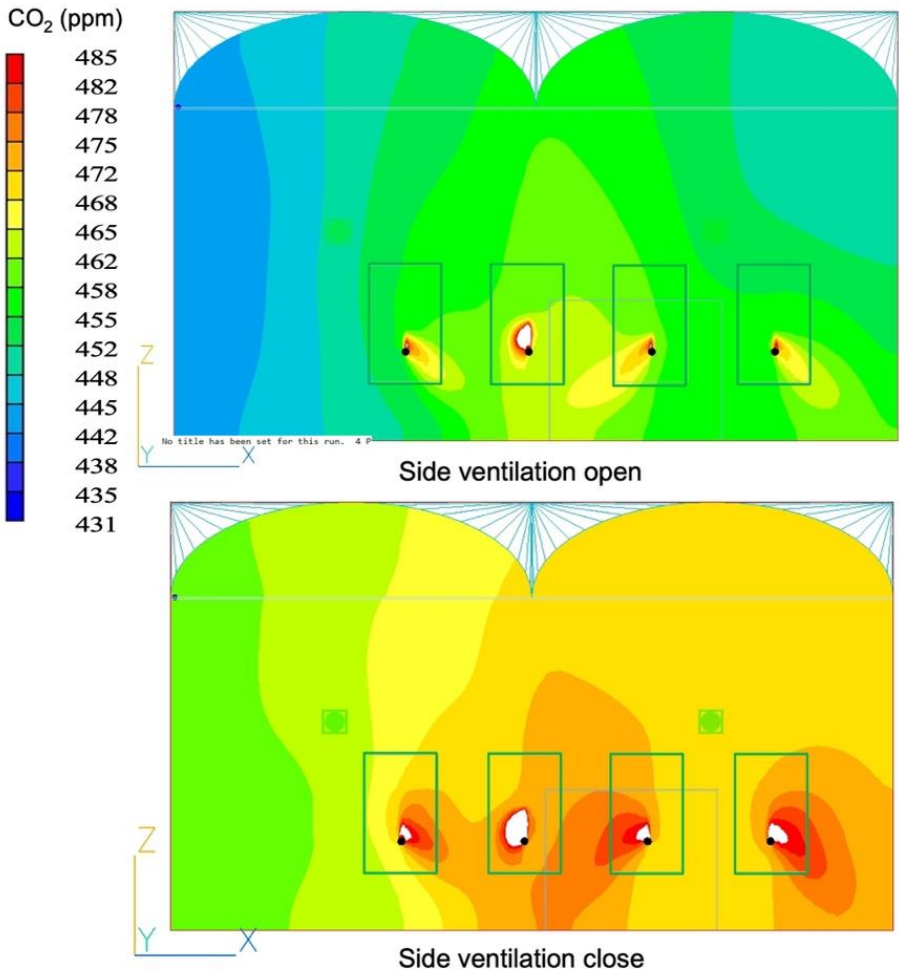

Figure 12. The CO_2 distribution inside of the greenhouse in case the side ventilations open and closed (image taken at cross-section 6 m from south wall).

When the sidewall was opened (ventilated), the inflow wind from outside the greenhouse was continually updated to match the current wind velocity in each mesh [33]. The CO_2 concentration outside of the greenhouse (400 ppm) is lower than the initial CO_2 concentration inside the greenhouse (450 ppm), which may cause the CO_2 concentration near the ventilated wall to be lower. Furthermore, the position of the plants in the greenhouse was asymmetric (tend to the right side).

The effects of open side vents on CO_2 distribution were slightly significant, especially near the wall. In comparison to the case of open side vents, the case with closed side vents showed a slightly more uniform CO_2 concentration within the greenhouse. Although the

side vents are closed, air circulators supported moving large volumes of air to provide even distribution. The quantitative evaluation of these results using CV shown in Table 5 is 18.2% for the open and 15.6% for the closed side vents case for the whole greenhouse.

Table 5. Coefficient of variations of CO_2 concentration in the case of side vents open and closed.

Parameter	Greenhouse		Plants	
	Side Vent			
	Open	Closed	Open	Closed
SD (ppm) [1]	80	71	41	41
Mean (ppm)	438	457	464	476
CV (%) [2]	18.2	15.6	8.8	8.7

[1] SD = Standard Deviation; [2] CV = Coefficient of variation.

However, focusing on the variability of CO_2 concentration inside the plant, open (8.8%) and closed (8.7%) side vents produced essentially no substantial contribution to even the variation of CO_2 concentration in the plant canopy because no initial wind velocity was considered at both side vents in our case. Therefore, virtually no air exchange occurred between outside and inside the greenhouse.

Figure 12 (side ventilation open) showed the CO_2 concentration around the plant (rectangular shapes) was still maintained higher than ambient CO_2 concentration (approximately 400 ppm). This suggests that practical CO_2 enrichment was still effective even if side vent was open (in case, no outside wind).

3.2.2. CO_2 Distribution toward on Sunny and Rainy Day Inside the Greenhouse

Simulations under treatment of 1000 ppm of CO_2 concentration, that had been done in the previous study [34,35] were conducted on a rainy day condition with PAR of 95 W m^{-2} [36] and sunny day condition with PAR of 355 W m^{-2} (based on NEDO solar radiation database).

There was a minor change in the CO_2 concentration between sunny and rainy days, according to the CO_2 distribution (Figure 13). The effects of solar radiation on CO_2 distribution were slightly significant. The case of rainy day showed a slightly more even of CO_2 distribution inside the greenhouse than the case of sunny day. For the entire greenhouse, the quantitative evaluation of these results using CV shown in Table 6 is 18.1% for the sunny-day case and 15.6% for the rainy-day case. However, when it comes to the variability of CO_2 concentration inside the plant, sunny day (8.1%) and rainy day (8.7%) had essentially no effect on even the fluctuation of CO_2 concentration in the plant canopy.

Table 6. Coefficient of variations of CO_2 concentration in the case of sunny and rainy day.

Parameter	Greenhouse		Plants	
	Weather			
	Sunny	Rainy	Sunny	Rainy
SD (ppm)	81	71	38	41
Mean (ppm)	446	457	467	476
CV (%)	18.1	15.6	8.1	8.7

Figure 14 shows the net photosynthesis estimations of the greenhouse model under treatment of 1000 ppm of CO_2 enrichment on a sunny and rainy day. The simulation results of a rainy and sunny days revealed the mean values of net photosynthesis (PCFD) of 3.82 and 9.69 μmol m^{-3} s^{-1}, respectively. The value of the net photosynthesis results seemed reasonable according to the study of Nederhoof and Vegter [29] and Xu et al. [37].

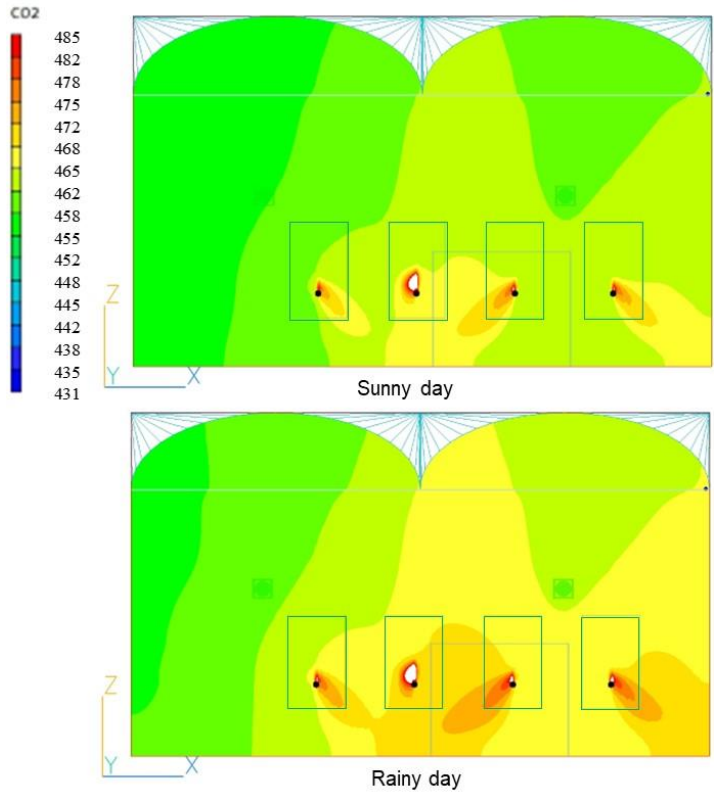

Figure 13. The CO_2 distribution inside of the greenhouse in case the sunny and rainy day (image taken at cross-section 6 m from south wall).

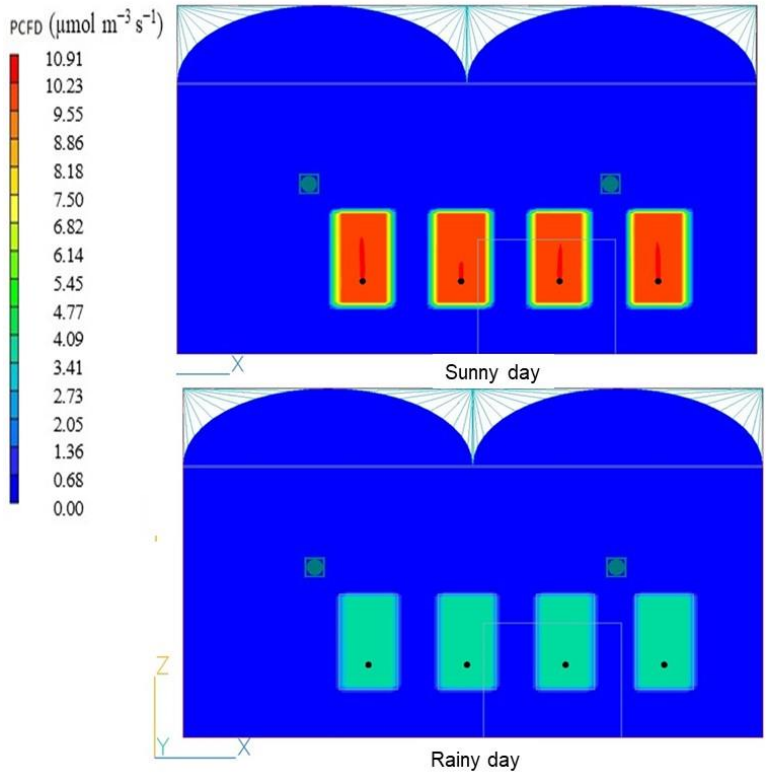

Figure 14. Net photosynthetic (PCFD) inside the greenhouse: 1000 ppm of CO_2 enrichment cases on sunny and rainy day.

The PAR possibly compensated the CO_2 absorption through the photosynthesis process to be low at low light (rainy day) and was higher at high light (sunny day). Nevertheless, the different canopy layers such as the top layer (64%), middle layer (28%), and bottom layer (8%) were not assigned to the net photosynthesis as mentioned in the study by Reichrath et al. [38] because in this simulation the dense of leaves were assumed to be homogenous for the whole plant. Thus, the net photosynthesis results were almost constant for the entire plant. However, according to the simulation results, this model may be appropriate to estimate the net photosynthesis average.

The variability of CO_2 concentration inside the plant between a rainy and a sunny day determined practically no significant difference. Furthermore, these models revealed no significant connection PAR and even the variation in CO_2 content at the plants.

3.3. Discussion

The study presented numerically the details of CO_2 distribution inside the chamber and the greenhouse. The performance of model was validated by comparing measurement and simulation results obtained from CFD model considering photosynthesis model. The model reproduced the distribution of measured CO_2 concentration in the middle of plant, decreasing due to CO_2 absorption by photosynthesis. As proven by Molina-Aiz et al. [9], the CFD model could simulate photosynthesis accurately.

The chamber simulation results at the bottom of plant showed good agreement with the measurement results. The middle and upper left cross sections of the canopy showed that the simulation results were overestimated. This is likely due to the fact that the turbulence intensity near the fan located at the top of the chamber tends to be stronger than in other parts of the chamber, and thus the CO_2 concentration near the fan tends to be lower due to turbulent mixing.

Otherwise, turbulence at the right side of the chamber is small (laminar), and because the simulation adopted a laminar model, the simulation achieved a better agreement with measurement for right side of the chamber.

The greenhouse simulation results at the bottom of canopy showed good agreement with the measurement results. In position of 3.4 m from north wall showed simulation results were overestimated. The position of 3.4 m from the south wall showed simulation results that were slightly underestimated for heights of 1.2 and 2.4 m from the ground, while the results for heights of 1.8 and 4.2 m from the ground were overestimated.

This may be because the temperature condition was neglected in the simulation. As reported by Kim et al. [14] that unequal distribution of CO_2 depends on temperature and location. However, the simulation was still able to predict the detailed of CO_2 distribution considering CO_2 absorption at the plant by photosynthesis and the error values were still reasonable compared to previous study [9,11].

A few simulations of greenhouse were conducted to know the effect of various environmental conditions to the CO_2 distribution inside of the greenhouse. Cases with open and closed side vents showed that closed side vents have slightly more even of CO_2 concentration than those with open side vents inside the greenhouse. In contrast, the variability of CO_2 inside the plant, open (8.8%) and closed (8.7%) side vents, induced almost no significant improvement.

Additionally, cases of a rainy- and sunny-day model showed that photosynthetically active radiation possibly compensated CO_2 absorption through photosynthesis to be lower at low light (rainy day) and higher at high light (sunny day). Nonetheless, we found that there was almost no significant difference in the variation of CO_2 concentration in the plant between rainy and sunny days.

4. Conclusions

The distribution of CO_2 in the chamber and greenhouse was studied to understand the details of CO_2 concentration while considering the net photosynthesis. Consequently, the measurement and simulation values of the CO_2 concentration were well-validated. We

determined that there would be no discernible difference in the CO_2 distribution between models with open and closed side vents of the greenhouse if there was no interference of air exchange for side vents. This study enables the prediction of net photosynthetic value concerning different PARs (rainy and sunny days).

The results showed that the average of net photosynthesis on a sunny day (9.69 μmol m^{-3} s^{-1}) was higher than on a rainy day (3.82 μmol m^{-3} s^{-1}). The link between the variability of CO2 concentration at the plants and the weather (sunny and rainy days), particularly PAR, did not appear to be significant. We determined that light and CO_2 distribution have an impact on the processes involved in photosynthesis. Thus, this research could take a role supporting agriculture technology.

In further research, an increase in the number of measurements would elucidate the CO_2 distribution considering photosynthesis. These could lead to a more accurate CFD model. Applying more parameters leads to simulation close to reality. To evaluate the photosynthetic model, consider the light distribution is based on the density of the canopy plant's leaves. Therefore, expanding the experiments on greenhouse microclimate, which includes photosynthesis and transpiration in different crops in the greenhouse would be of importance.

Author Contributions: Conceptualization, M.N. and T.T.; methodology, M.N.; chamber and greenhouse simulations, M.N. and T.T.; validation, M.N.; writing—original draft preparation, M.N.; writing—review and editing, T.T.; greenhouse investigation, T.K.; supervision, T.I. and K.T. All authors have read and agreed to the published version of the manuscript.

Funding: This research was partially funded by "Knowledge Hub Aichi", Priority Research Project from Aichi Prefectural Government, and also by a grant from a commissioned project study on "AI-based optimization of environmental control and labor management for large-scale greenhouse production", Ministry of Agriculture, Forestry and Fisheries, Japan.

Institutional Review Board Statement: Not applicable.

Informed Consent Statement: Not applicable.

Data Availability Statement: Not applicable.

Acknowledgments: The first author appreciates MEXT and AMANO for the support through scholarship of doctoral degree. The authors also would like to thanks to Seitaro Toda in Toyohashi University of Technology for the technical support with our measurements.

Conflicts of Interest: The authors declare no conflict of interest.

References

1. Zhang, Y.; Kacira, M.; An, L. A CFD study on improving air flow uniformity in indoor plant factory system. *Biosyst. Eng.* **2016**, *147*, 193–205. [CrossRef]
2. Benni, S.; Tassinari, P.; Bonora, F.; Barbaresi, A.; Torreggiani, D. Efficacy of greenhouse natural ventilation: Environmental monitoring and CFD simulations of a study case. *Energy Build.* **2016**, *125*, 276–286. [CrossRef]
3. Santolini, E.; Pulvirenti, B.; Benni, S.; Barbaresi, L.; Torreggiani, D.; Tassinari, P. Numerical study of wind-driven natural ventilation in a greenhouse with screens. *Comput. Electron. Agric.* **2018**, *149*, 41–53. [CrossRef]
4. Roy, J.C.; Boulard, T.; Kittas, C.; Wang, S. Convective and ventilation transfers in greenhouses, part 1: The greenhouse considered as a perfectly stirred tank. *Biosyst. Eng.* **2002**, *83*, 1–20. [CrossRef]
5. Kim, R.W.; Lee, I.B.; Kwon, K.S. Evaluation of wind pressure acting on multi-span greenhouses using CFD technique, Part 1: Development of the CFD model. *Biosyst. Eng.* **2017**, *164*, 235–256. [CrossRef]
6. Kichah, A.; Bournet, P.E.; Migeon, C.; Boulard, T. Measurement and CFD simulation of microclimate characteristics and transpiration of an Impatiens pot plant crop in a greenhouse. *Biosyst. Eng.* **2012**, *112*, 22–34. [CrossRef]
7. Fang, H.; Li, K.; Wu, G.; Cheng, R.; Zhang, Y.; Yang, Q. A CFD analysis on improving lettuce canopy airflow distribution in a plant factory considering the crop resistance and LEDs heat dissipation. *Biosyst. Eng.* **2020**, *200*, 1–12. [CrossRef]
8. Roy, J.C.; Pouillard, J.B.; Boulard, T.; Fatnassi, H.; Grisey, A. Experimental and CFD results on the CO_2 distribution in a semi closed greenhouse. *Acta Hortic.* **2014**, *1037*, 993–1000. [CrossRef]
9. Molina-Aiz, F.D.; Norton, T.; López, A.; Reyes-Rosas, A.; Moreno, M.A.; Marín, P.; Espinoza, K.; Valera, D.L. Using computational fluid dynamics to analyse the CO_2 transfer in naturally ventilat0ed greenhouses. *Acta Hortic.* **2017**, *1182*, 283–292. [CrossRef]

10. Niam, A.G.; Muharam, T.R.; Widodo, S.; Solahudin, M.; Sucahyo, L. CFD simulation approach in determining air conditioners position in the mini plant factory for shallot seed production. In Proceedings of the 10th International Meeting of Advances in Thermofluids, Bali, Indonesia, 16–17 November 2018. [CrossRef]
11. Zhang, Y.; Yasutake, D.; Hidaka, K.; Kitano, M.; Okayasu, T. CFD analysis for evaluating and optimizing spatial distribution of CO_2 concentration in a strawberry greenhouse under different CO_2 enrichment methods. *Comput. Electron. Agric.* **2020**, *179*, 105811. [CrossRef]
12. Li, Y.; Ding, Y.; Li, D.; Miao, Z. Automatic carbon dioxide enrichment strategies in the greenhouse: A review. *Biosyst. Eng.* **2018**, *171*, 101–119. [CrossRef]
13. Kuroyanagi, T.; Yasuba, K.; Higashide, T.; Iwasaki, Y.; Takaichi, M. Efficiency of carbon dioxide enrichment in an unventilated greenhouse. *Biosyst. Eng.* **2014**, *119*, 58–68. [CrossRef]
14. Kim, C.H.; Kim, M.H.; Choi, E.G.; Jin, B.O.; Baek, G.Y.; Yoon, Y.C.; Kim, H.T. CO_2 distribution due to thermal buoyancy in the greenhouse. In Proceedings of the 5th International Federation of Automatic Control on Biorobotics, Sakai, Japan, 27–29 March 2013. [CrossRef]
15. Shimomoto, K.; Takayama, K.; Takahashi, N.; Nishina, H.; Inaba, K.; Isoyama, Y.; Oh, S.C. Real-time monitoring of photosynthesis and transpiration of a fully-grown tomato plant in greenhouse. *Environ. Control Biol.* **2020**, *58*, 65–70. [CrossRef]
16. Campen, J.B. Greenhouse design applying CFD for Indonesian conditions. *Acta Hortic.* **2005**, *691*, 419–424. [CrossRef]
17. Wang, X.W.; Luo, J.Y.; Li, X.P. CFD based study of heterogeneous microclimate in a typical chinese greenhouse in central China. *J. Integr. Agric.* **2013**, *12*, 914–923. [CrossRef]
18. Boulard, T.; Roy, J.C.; Pouillard, J.B.; Fatnassi, H.; Grisey, A. Modelling of micrometeorology, canopy transpiration and photosynthesis in a closed greenhouse using computational fluid dynamics. *Biosyst. Eng.* **2017**, *158*, 110–133. [CrossRef]
19. Kuroyanagi, T. Prediction of leakage rate of a greenhouse using computational fluid dynamics. *Acta Hortic.* **2017**, *1170*, 87–94. [CrossRef]
20. Hong, S.W.; Exadaktylos, V.; Lee, I.B.; Amon, T.; Youssef, A.; Norton, T.; Berckmans, D. Validation of an open source CFD code to simulate natural ventilation for agricultural buildings. *Comput. Electron. Agric.* **2017**, *138*, 80–91. [CrossRef]
21. Saberian, A.; Sajadiye, S.M. The effect of dynamic solar heat load on the greenhouse microclimate using CFD simulation. *Renew. Energy.* **2019**, *138*, 722–737. [CrossRef]
22. Bouhoun, A.H.; Bournet, P.E.; Cannavo, P.; Chantoiseau, E. Development of a CFD crop submodel for simulating microclimate and transpiration of ornamental plants grown in a greenhouse under water restriction. *Comput. Electron. Agric.* **2018**, *149*, 26–40. [CrossRef]
23. Boulard, T.; Wang, S. Experimental and numerical studies on the heterogeneity of crop transpiration in a plastic tunnel. *Comput. Electron. Agric.* **2002**, *34*, 173–190. [CrossRef]
24. Majdoubi, H.; Boulard, T.; Fatnassi, H.; Bouirden, L. Airflow and microclimate patterns in a one-hectare Canary type greenhouse: An experimental and CFD assisted study. *Agric. For. Meteorol.* **2009**, *149*, 1050–1062. [CrossRef]
25. Zhang, Y.; Wei, Z.; Xu, J.; Wang, H.; Zhu, H.; Lv, H. Numerical simulation and application of micro-nano bubble releaser for irrigation. *Mater. Express* **2021**, *11*, 1007–1015. [CrossRef]
26. Kumazaki, T.; Ikeuchi, Y.; Tokairin, T. Relationship between positions of CO_2 supply in a canopy of tomato grown by high-wire system and distribution of CO_2 concentration in a greenhouse. *Clim. Biosph.* **2021**, *21*, 54–59. [CrossRef]
27. PHOENICS User Manual. The Mathematical Basis of PHOENICS. Available online: https://www.cham.co.uk/phoenics/d_polis/d_lecs/general/maths.htm (accessed on 18 February 2022).
28. Stathopoulou, O.I.; Assimakopoulos, V.D. Numerical study of the indoor environmental conditions of a large athletic hall using the CFD code PHOENICS. *Environ. Model. Assess.* **2008**, *13*, 449–458. [CrossRef]
29. Nederhoff, E.M.; Vegter, J.G. Canopy photosynthesis of tomato, cucumber, and sweet pepper in greenhouses: Measurements compared to models. *Ann. Bot.* **1994**, *73*, 421–427. [CrossRef]
30. Nurmalisa, M.; Tokairin, T.; Takayama, K.; Inoue, T. Numerical simulation of detailed airflow distribution in newly developed photosynthesis chamber. In Proceedings of the 2nd International Conference on Environment, Sustainability Issues, and Community Development (Virtual Conference), Semarang, Indonesia, 21 October 2020. [CrossRef]
31. Kuroyanagi, T. Investigating air leakage and wind pressure coefficients of single-span plastic greenhouses using computational fluid dynamics. *Biosyst. Eng.* **2017**, *163*, 15–27. [CrossRef]
32. Velázquez, J.F.; Gea, G.D.T.; Garcia, E.R.; Cruz, I.L.L.; Aguilar, A.R. Advances in Computational Fluid Dynamics Applied to the Greenhouse Environment. In *Applied Computational Fluid Dynamics*; Oh, H.W., Ed.; IntechOpen: London, UK, 2012; pp. 35–62. [CrossRef]
33. PHOENICS User Manual. VR Object Types and Attributes. Available online: https://www.cham.co.uk/phoenics/d_polis/d_docs/tr326/obj-type.htm (accessed on 20 February 2022).
34. Nederhoff, E.M.; Vegter, J.G. Photosynthesis of stands of tomato, cucumber, and sweet pepper measured in greenhouses under various CO_2 concentrations. *Ann. Bot.* **1994**, *73*, 353–361. [CrossRef]
35. Kim, H.T.; Kim, C.H.; Choi, E.G.; Jin, B.O.; Yoon, Y.C.; Kim, H.T. The effect of thermal conditions on CO_2 distribution in a greenhouse. *Trop. Agric. Res.* **2015**, *26*, 714. [CrossRef]

36. Romdhonah, Y.; Fujiuchi, N.; Shimomoto, K.; Takahashi, N.; Nishina, H.; Takayama, K. Averaging techniques in processing the high time-resolution photosynthesis data of cherry tomato plants for model development. *Environ. Control Biol.* **2021**, *59*, 107–115. [CrossRef]
37. Xu, S.; Zhu, X.; Li, C.; Ye, Q. Effects of CO_2 enrichment on photosynthesis and growth in Gerbera jamesonii. *Sci. Hortic.* **2014**, *177*, 77–84. [CrossRef]
38. Reichrath, S.; Ferioli, F.; Davies, T.W. A simple computational fluid dynamics (CFD) model of a tomato glasshouse. *Acta Hortic.* **2000**, *534*, 197–202. [CrossRef]